Highly Efficient Wideband mmWave Rectennas for Wireless Power Transfer System with Low-Cost Multi-Node Tracking Capability

Chaoyun Song, *Senior Member, IEEE*, Lei Wang, *Senior Member, IEEE*, Ping Lu, *Member, IEEE,* Cheng Zhang*, Member, IEEE,* Zhensheng Chen, Xuezhi, Zheng*, Member, IEEE*, Yejun He, *Senior Member, IEEE,* George Goussetis, *Senior Member, IEEE,* Guy A. E. Vandenbosch, *Fellow, IEEE* and Yi Huang, *Fellow, IEEE*

***Abstract*—An innovative wireless power transfer (WPT) system utilizing millimeter wave (mmWave) power for multi-node charging and tracking is presented in this paper. The core concept of the system revolves around the utilization of frequency-dispersive leaky-wave antenna transmitters, enabling passive beam scanning in the far-field without the need for active phased arrays. However, such a system requires a breakthrough in receiving rectenna design at mmWave frequencies, encompassing a wide frequency bandwidth, wide beam width, and high RF-DC conversion efficiency beyond 20 GHz. In this work, we introduce a pioneering mmWave rectenna design achieved through the co-design integration of a magnetoelectric dipole and high-frequency diodes, eliminating the need for complex impedance matching networks at mmWave frequencies. The proposed rectenna operates in the frequency range of 24-34.5 GHz, achieving over 50% RF-DC conversion efficiency for input powers exceeding 15 dBm. Additionally, the rectenna demonstrates improved gain and beamwidth compared to conventional designs, enabling wide-angle reception of frequency-scanning passively beamformed mmWave signals. A practical demonstration of the proposed system showcases simultaneous wireless charging of three nodes, highlighting its notable advantages in terms of mobility, cost-effectiveness, and simplicity over conventional WPT technologies.**

***Index Terms*—leaky-wave antenna, mmWave, node tracking, rectennas, wireless power transfer.**

I. Introduction

WIRELESS power transfer (WPT) has a transformative potential to simplify our everyday life as it increases mobility, convenience, and safety for plenty of applications in consumer electronics, electric vehicles, defense and space technologies [1]. The development of WPT technology has been historically important, which started with Tesla's heritage experiment in the 1890s, and has experienced an over 100 years' roadmap with many significant achievements and milestones [2-6]. In recent decades, the emergence of the Qi standard in 2010 enabled vast ranges of smartphones and wearable devices with wireless charging capabilities [7-8]. But user benefits largely rely on the elimination of cords and wires but fall short of providing the flexibility of truly remote (charging distance >20 cm) and on-the-move charging of handheld devices. The hunt for remote and on-the-move charging is on [9].

Far-field WPT via radio waves is a promising way for remote charging (e.g., up to kilometers for Space Solar Power Satellites [10]). However, the radiative wireless power could be largely scattered in open areas whilst the path loss of radio waves propagating in free space is significant; consequently, the end-to-end efficiency of the far-field WPT system is relatively low. This has been the main challenge for traditional radiative power transfer. To improve the WPT link efficiency, high directivity antenna arrays with beamforming capabilities are preferred to transmit power effectively. State-of-the-art research has shown the feasibility of using the phased array [11-15] and digital meta-surfaces [16-18] for wireless power beamforming and near-field beam focusing, such that the power beam could be focused sharply while the beam direction is switchable toward several receiver locations. But the phased array concept essentially needs active phase shifters and array feeding networks which introduces significant power loss (more than 6 dB) and increases the costs tremendously. Similarly, digital meta-surface and beamformers for radiative near-field focusing needs the massive integration of PIN diodes and costly semiconductor varactors thereby reducing the WPT efficiency and charging distances. The beam scanning range, the number of beam directions and the beam scanning resolution of both technologies are directly determined by how many active phase shifters and switches are integrated into the design. These significant drawbacks in terms of high complexity, high power loss, and high cost have become the bottleneck when applying such far-field WPT in real-world applications.

Node tracking is crucial when wirelessly remote charging a moving target. This will need the feedback information sent from the receiver to effectively control the wireless power beamforming at the transmitter. Existing studies have

Manuscript received 19 July 2023, revised 29 August 2023. This work was supported in part by the King's College London (KCL) starting grant, in part by the National Natural Science Foundation of China (NSFC) under Grant 62071306, in part by Shenzhen Science and Technology Program under Grants JCYJ20200109113601723, JSGG20210802154203011 and JSGG20210420091805014.

C. Song is with the Department of Engineering, King's College London, Strand Campus, London, WC2R 2LS, U.K. (chaoyun.song@kcl.ac.uk)

L. Wang, and G. Goussetis are with the School of Engineering and Physical Sciences, Heriot-Watt University, Edinburgh EH14 4AS, Scotland, UK.

P. Lu is with the School of Electronics and Information Engineering, Sichuan University, Chengdu 610064, China.

C. Zhang is with Shanghai Institute of Optics and Fine Mechanics, Chinese Academy of Sciences, Shanghai 201800, China.

Z. Chen X. Zheng, and G. A. E. Vandenbosch are with Department of Electrical Engineering (ESAT), KU Leuven, 3001 Leuven, Belgium.

C. Song and Y. He are with State Key Laboratory of Radio Frequency Heterogeneous Integration (Shenzhen University), College of Electronics and Information Engineering, Shenzhen University, Shenzhen 518060, China.

Y. Huang is with the Department of Electrical Engineering and Electronics, University of Liverpool, Liverpool L69 3BX, U.K.

demonstrated the use of retrodirective antenna arrays (RDA) for node tracking [19, 20]. An RDA automatically retransmits a signal towards a source without prior knowledge of the incoming signal. Due to the need for phase conjugation to realize retro-directivity, RDAs typically consist of signal mixers, sub-arrays and multiple power amplifiers (PAs) and bandpass filters [19]. This might bring in extra costs, power loss and complexity for the WPT systems. Time reversal (TR) is another emerging technology for selectively delivering wireless power to the targeted nodes. Different from the phased array that relies on phase shifting, TR transmitting arrays operate in a switching manner where only one element transmits at a time [21, 22]. The node selectivity is accomplished by measuring the feedback beacon signal sent from the receiver and correspondingly selecting the optimal transmitting antenna element. But both RDA and TR technologies need large active antenna arrays consisting of multiple antenna elements, PAs and complex feedings. They still need to be actively controlled and/or switched which inherently has a higher cost and higher power loss compared to the conventional passive transmitting antenna.

Therefore, having considered all state-of-the-art technologies, the major challenges for far-field radiative WPT are summarized as follows. 1) How to increase the WPT efficiency and power delivery at larger distances? 2) How to enable node-tracking and beamforming for the WPT system with low-cost and low-power loss methods? 3) How to effectively establish a multi-target WPT system with excellent simplicity, cost-effectiveness, and reliability?

To address these grand challenges, in this paper, we will present a brand-new wireless power transfer system using mmWave signals. The benefits of mmWave WPT in terms of relaxed EIRP level, higher efficiency and higher deliverable power will be introduced in Section II. Importantly, we will propose a novel passive beamforming method by exploiting the inherent frequency dispersion nature of leaky wave antenna transmitters [34, 35], thereby eliminating the need for active phased array transmitters which exhibit extremely high cost and high-power loss at mmWave frequencies.

At the receiver end, we will present a newly designed wideband and wide-beam mmWave rectenna to efficiently capture the spectrum-sweeping signals transmitted from the leaky-wave antenna (Section III). It is worth noting that wideband mmWave rectennas with high conversion efficiency have not been widely reported [23, 24]. Only a limited number of works have demonstrated good power conversion efficiency exceeding 30% and wide bandwidth [25-31]. In this paper, we conduct an in-depth theoretical and experimental investigation of the co-designing strategy involving a magnetoelectric dipole and high-frequency diodes over a wide mmWave spectrum from 20 to 40 GHz, thereby for the first time reporting a highly efficient (>50%), wide beamwidth (>90 degrees) and wideband (34.5% bandwidth) mmWave rectenna. Experimental verification of the proposed mmWave rectenna is presented in Section IV.

Antenna size: Transmitting: 20 cm Receiving: 4 cm WPT distance: 5 m	Conventional microwave WPT (at 3 GHz)	The Proposed mmWave WPT (at 30 GHz)	Improvement rate (dB or %)
TX antenna gain	13 dBi	30 dBi	17 dB
RX antenna gain	2 dBi	10 dBi	8 dB
EIRP Limit	36 dBm	75 dBm	39 dB
Max. TX power	23 dBm	45 dBm	22 dB
Max. RX power	-18 dBm	9 dBm	27 dB
WPT efficiency	$7.5X10^{-3}$ %	$2.5X10^{-2}$ %	333%
Path Loss	41 dB	36 dB	5 dB
Beam scanning loss	>6 dB	0 dB	6 dB

Fig. 1. Comparison between conventional WPT system at 3 GHz and the proposed WPT system at 30 GHz. Note that the WPT efficiency here is the RF-RF power transfer efficiency at 5 m without considering the rectification.

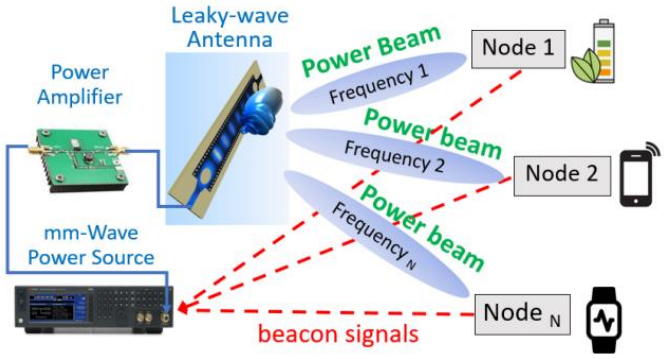

Fig. 2. Proposed multi-target WPT system using mmWave power. The system consists of a leaky-wave antenna (LWA), power amplifier (PA), signal source and mmWave wideband wide-beam rectennas. The feedback beacon signal is used for multi-node tracking.

Moreover, a preliminary demonstration for the proposed multi-target wireless charging and node tracking system is showcased in Section V. Three nodes can be wirelessly powered simultaneously with a closed control loop using the DC power monitor for the rectenna, feedback beacon signals and multi-frequency modulation and sweeping for the transmitting mmWave signals. Finally, conclusions are drawn in Section VI.

II. Wideband mmWave Wireless Power Transfer

A. *Why mmWave?*

Compared to sub-6 GHz bands, the EIRP (Effective Isotropic Radiated Power) limit of mmWave band is increased from 36 dBm to 75 dBm (according to FCC and 3GPP) [26]. This means that the mmWave power transmitter could radiate significantly enhanced power (about 39 dB higher) in domestic environments within safety human exposure constraints. In addition, mmWave antennas offer the advantage of achieving higher directivity (> 25 dBi) with a given aperture size. Furthermore, mmWave RF devices naturally have smaller overall dimensions compared to microwave devices. For instance, the wavelength at 3 GHz is ten times larger than that at 30 GHz, resulting in a reduced physical size of mmWave devices. Hence, a high directivity mmWave WPT system may have better end-to-end efficiency as well as much higher

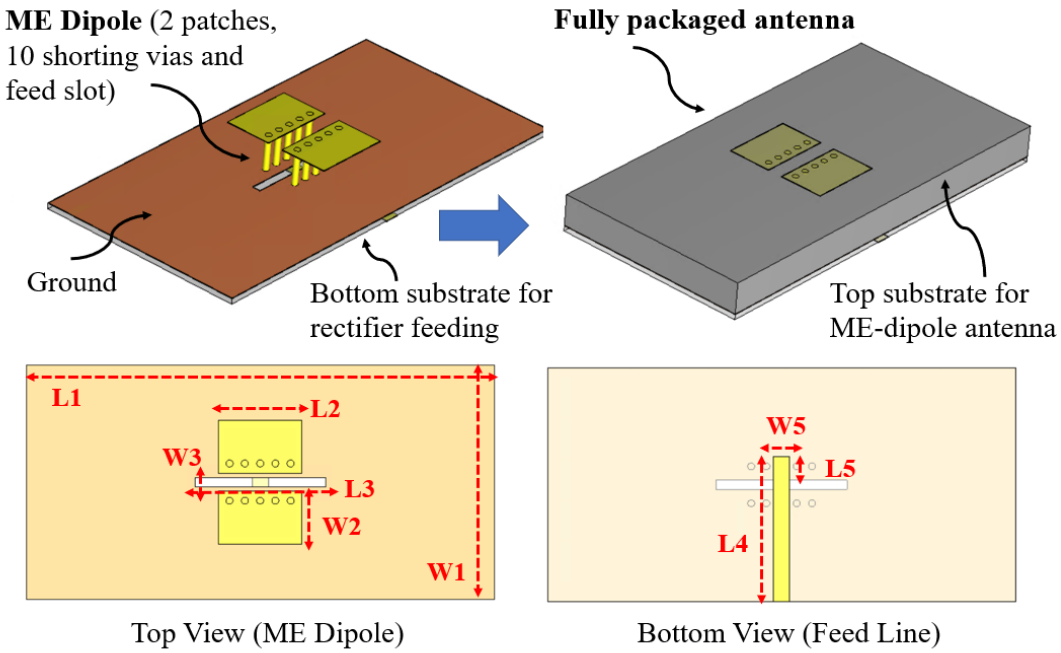

Fig. 3. Proposed wideband mmWave ME-dipole for antenna and rectifier codesign. The antenna is produced on high frequency RT5880 substrate with a thickness of 1.575 mm and the feed line is produced on the same material with a thickness of 0.254 mm, which is attached to the bottom. List of parameters: L1 = 20 mm, W1 = 10 mm, L2 = 3.56 mm, W2 = 2.25 mm, L3 = 5.6 mm, W3 = 0.4 mm, L4 = 6.2 mm, L5 = 1.2 mm, W5 = 0.7 mm. The via holes are metallized holes with a diameter of 0.3 mm, and a gap (center to center) of 0.65 mm.

deliverable wireless power at identical distances compared with microwave systems. In Fig. 1, we have compared the performance of a typical WPT system at 3 GHz with that of our proposed system at 30 GHz. We assume both systems have an identical transmitting aperture side of 20 cm and a receiving aperture size of 4 cm. The conventional 3 GHz system was estimated using microstrip patch antenna array [32]. At an identical power transfer distance of 5 m, the proposed mmWave system will have 27 dB more received power, 5 dB less path loss and 333% efficiency improvement. The free space path loss can be greatly mitigated by high directivity and high aperture efficiency of mmWave antennas whilst the transmitting power is enhanced by the relaxed EIRP regulations. However, the major challenges for mmWave WPT the cost, power loss and efficiency of mmWave PAs, phase shifters and active switches. It is overly expensive to build the power beamforming and node tracking capabilities for the remote charging system at mmWave frequencies using conventional technologies and for this reason, it has not yet been substantially explored [33]. The active beam scanning loss (e.g., phased array) at 3 GHz will be more than 6 dB and it will be even higher at 30 GHz.

B. Novelty and Advantages

The proposed system architecture is illustrated in Fig. 2. In this study, our focus is on utilizing a passive beam-scannable and beam-formable antenna called the leaky-wave antenna (LWA). The LWA is a type of travelling-wave antenna that relies on a guiding structure to support wave propagation along its length, with the wave continuously or periodically radiating/leaking along the structure. It exhibits natural frequency-dependent beam scanning and exceptional radiation efficiency (>90%) at mmWave frequency bands [34, 35]. Although the frequency-dispersive nature of the LWA presents challenges in typical wireless communications, we can leverage this characteristic for wireless power transfer (WPT). Specifically, we can develop a wideband wide-beam rectenna (power receiver) capable of capturing frequency-dependent power beams emitted by the LWA transmitter. By employing this approach, beamforming of the LWA power transmitter can be accomplished simply by adjusting the frequency of the mmWave signals. This approach offers significant advantages over conventional active beam scanning, near-field focusing, and other WPT beamforming methods, including reduced power loss, cost, and complexity. In our proposed system, multi-target tracking can be achieved through multi-tone frequency modulation and sweeping, with real-time control based on feedback signals received from the rectennas.

The core concept involves identifying the synchronized instance for delivering the peak DC power to the rectenna and shaping the power beam according to the frequency spectrum. Further details regarding this approach will be provided in Section V of the paper. However, it is evident that the primary challenge lies in designing highly efficient wideband and wide-beam rectennas for mmWave bands. This challenge forms the main focus of our research.

III. Wideband Wide-beam mmWave Rectenna Design

In the proposed WPT system, the receiving rectennas will undoubtedly become the most challenging part to be dealt with. One reason is due to the requirement for high RF-DC conversion efficiency across large frequency bandwidth to cope with the wide-angle scanning beams radiated from the frequency-scanning LWAs. Another critical concern is around

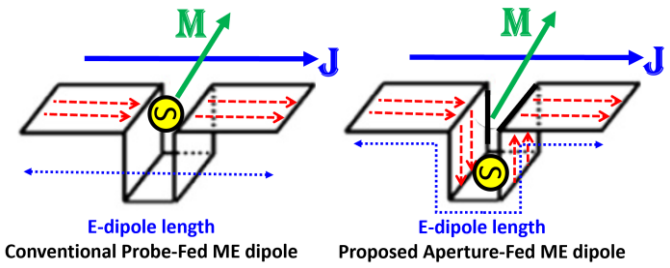

Fig. 4. Operating mechanism comparison between conventional probe-fed ME dipole and the proposed aperture-fed ME dipole. Red dashed line represents the surface current distribution on the electric-dipole arm.

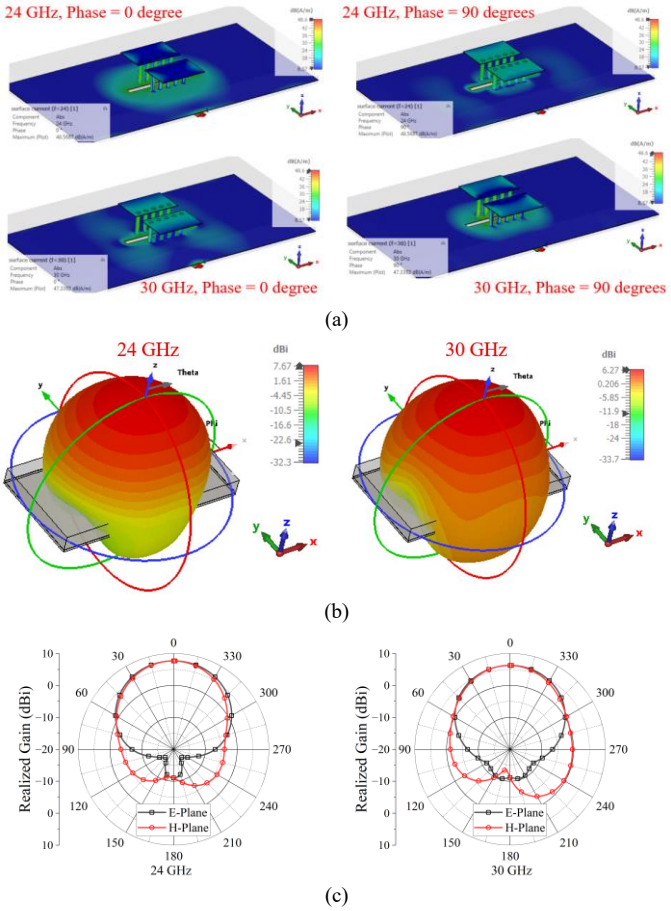

Fig. 5. (a) Surface current distribution, (b) 3D radiation pattern and (c) (c) 2D radiation pattern (over E-plane and H-plane) of the proposed ME dipole antenna at 24 and 30 GHz.

the trade-offs between half power beamwidth and directivity of the receiver, in which the broadband rectenna is ideally of high gain and wide beam. More importantly, the proposed antenna will need to operate at a wide mmWave spectrum for frequencies > 20 GHz, thereby posing significant challenges in terms of the rectifier design by using high-frequency diodes.

To date, there is a very limited number of mmWave rectennas published in the open literature whilst very few works can operate effectively over a large bandwidth. A valuable conclusion summarized from the existing work is that the rectifiers at mmWave frequency could be sensitive to the soldering and circuit elements, thus a promising direction to minimize the loss of mmWave rectifiers is to reduce the utilization of SMD devices and chip components, in which the matching, RF filtering and DC filtering circuit elements should have been transformed purely into printed transmission lines on a highly efficient substrate (e.g., RT5880) with low power loss. In addition, the antenna and rectifier could be co-designed to minimize the insertion loss caused by the impedance matching networks for a wide bandwidth over mmWave spectrums.

Hence, we will consider the development of a co-designed wideband rectenna, for the first time, at the mmWave frequencies with state-of-the-art conversion efficiency.

A. ME Dipole

Magnetoelectric (ME) dipole antenna has been demonstrated to have wide impedance bandwidth, wide beamwidth, and reasonably high gain for both microwave and mmWave frequency bands [36-39]. The complementary radiation originated from electric and magnetic dipoles could form a unidirectional pattern with a wide beamwidth of > 100 degrees. Therefore, we will employ ME dipole in the proposed rectenna design. Different from the conventional ME-dipole that only concerns its antenna characteristics, for the proposed rectenna design, the capability for circuit integration with PCB mmWave rectifier and antenna-to-rectifier codesign will also need to be carefully considered here.

Fig. 3 depicts the proposed ME dipole antenna that consists of 2 patches (electric dipole arm), 2×5 shorting vias and a feeding slot (magnetic dipole). The electric dipole is hosted by using a single layer of high-frequency RT5880 substrate (dielectric constant =2.1, loss tangent = 0.001 at 40 GHz) with a thickness of 1.575 mm. The printed patch dipole arms are linked electrically to the ground via 10 shorting pins on both patches, with a metallized hole diameter of 0.3 mm. The detailed dimensions for an optimized design covering 20– 32 GHz are given in the caption of Fig. 3. The overall size of the ME-dipole is $20 \times 10 \times 1.9\ mm^3$. It is noted that since antenna is aperture fed, a microstrip feed line is printed on a thin layer of RT5880 (thickness = 0.254 mm) and located on the bottom of the antenna. The operating principle of the proposed ME-dipole is depicted in Fig. 4 where the magnetic dipole is mainly determined by the feed slot. It is slightly different from the probe-fed ME-dipole where the electric dipole current does not travel along the shorted patch/vias [40]. While the probe-fed method has shown potential in reducing antenna height [41] and extending bandwidth [42], it is important to note that this approach often requires a more intricate structural design and the incorporation of shorting vias to facilitate the probe connection. This complexity can subsequently pose challenges for the seamless integration of rectifiers at the system level, particularly in the context of mmWave rectennas.

Fig. 5 shows the 3D/2D radiation pattern and surface current distribution of the proposed ME-dipole at 24 and 30 GHz. It can be seen that the surface current on the top patch and shorting vias flows along the desired current directions of an electric dipole (see Fig. 5(a)) whilst the surface current around the feeding slot is perpendicular to the electric dipole, thereby forming the magnetic dipole radiation. At phase = 0°, the horizontal current on the planar dipole is dominated where the currents with quasi-sinusoidal distribution on the electric

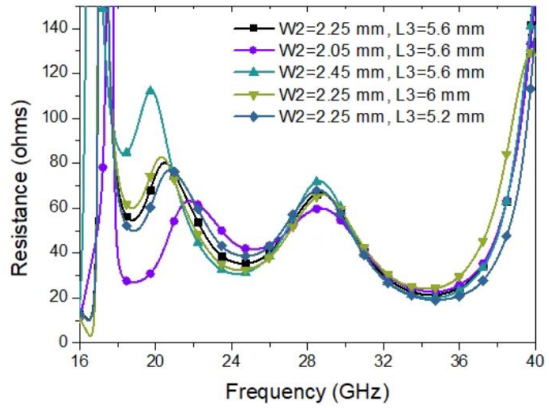

(a)

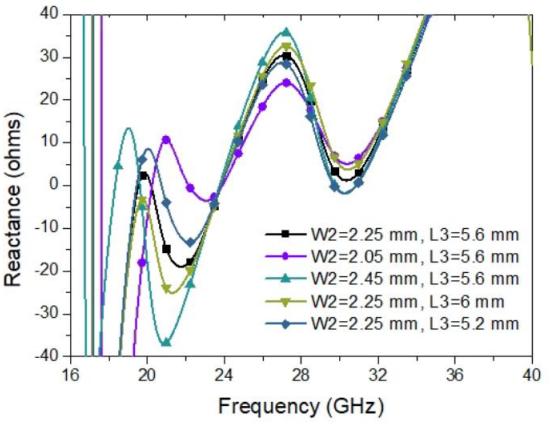

(b)

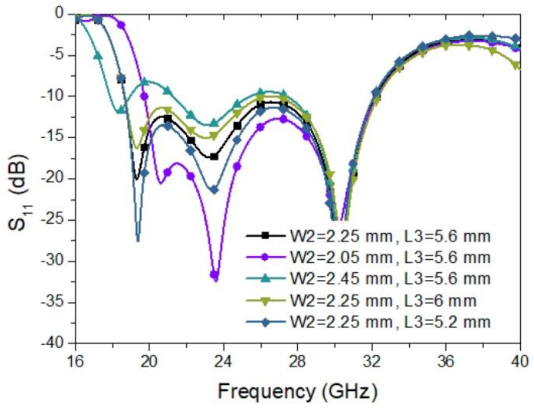

(c)

Fig. 6. (a) Read part (resistance) of the antenna impedance. (b) Imaginary part (reactance) of the antenna impedance. (c) Reflection coefficient of the proposed ME-dipole antenna for 50 ohms port impedance.

dipoles are found to be maximum. In contrast, at phase = 90° the horizontal currents and the aperture electric field are minimized, while vertical currents on the shorting pins are strongly excited. The antenna exhibits a unidirectional beam of > 90 degrees beamwidth and around 6.3 –7.7 dBi gain (e.g., Fig. 5(b)) with a very low backward radiation (see Fig. 5(c)) over the wide frequency band of interest.

For the antenna-to-rectifier codesign, it is crucial to analyze the antenna resonance and impedance, from a circuit point of view. The frequency dependence of the antenna/rectifier complex impedance could play an important role in the conjugate matching for wideband rectifiers if the antenna

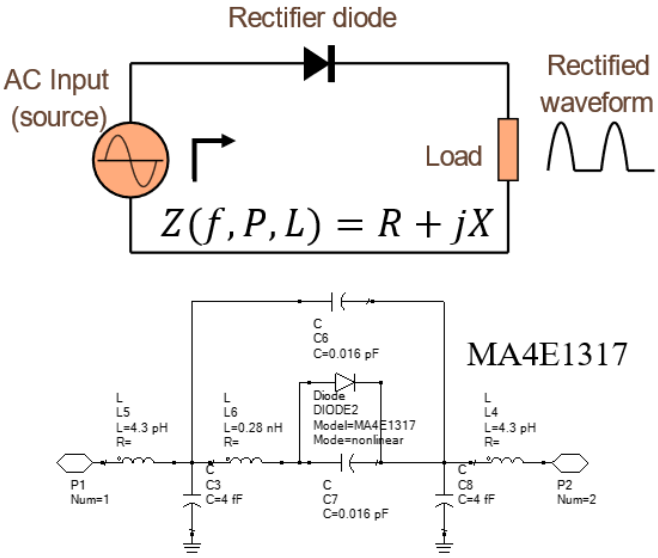

Fig. 7. mmWave diode behavior model and circuit diagram to evaluate its complex impedance variations against frequency, power and load.

impedance could be tuned strategically [39, 40]. The simulated complex impedance of the ME-dipole is shown in Figs. 6(a) and (b). Here we show examples of tuning two major parameters: W2 (electric dipole length) and L3 (magnetic dipole length). To help readers get a better understanding, the reflection coefficient calculated using 50 ohms port impedance is depicted in Fig. 6 (c). By adjusting the electric dipole, the antenna impedance varies significantly at around 20 GHz while the impedance will change at around 24 GHz when the magnetic dipole L3 is tuned. Such a freedom of impedance tuning could contribute to the conjugate impedance matching with nonlinear rectifier over a range of frequencies, powers and loads [43, 44].

Fig. 6 (a)-(c) shows that the proposed ME dipole is capable of achieving a wide impedance bandwidth over 20– 32 GHz (FBW =46%) for S_{11} < -10 dB and has an excellent capability for impedance tuning either inductively or capacitively to match the rectifiers over the aforesaid frequency band. Note that the S_{11} in Fig. 6(c) is for illustrative examples only, it might not be identical for the co-designed rectenna S_{11}, as the impedance of rectifying diode is a complex number and a nonlinear function of frequency, power and circuit loads.

B. Wideband mmWave Diode and Rectifier

For the mmWave rectifier design, the feed line from the ME dipole antenna could be used to link the rectifier on the printed substrate. Importantly, an accurate diode model becomes crucial to improve the precision and reliability of the overall rectifier/rectenna performance. Some work has considered modelling the mmWave diodes either using SPICE parameter-based behavior model [30, 47] or using experimental data matrix and real-time S parameter files [48]. It is generally concluded that the MA4E1317 diode could perform effectively up to 80 GHz with high conversion efficiency (>40%), if the mmWave rectifying circuit is properly designed.

For the diode modelling, here we employ model parameters of MA4E1317 that are extracted from the *I–V, C–V*, and small signal S-parameter measurements, as reported in [48]. Such a

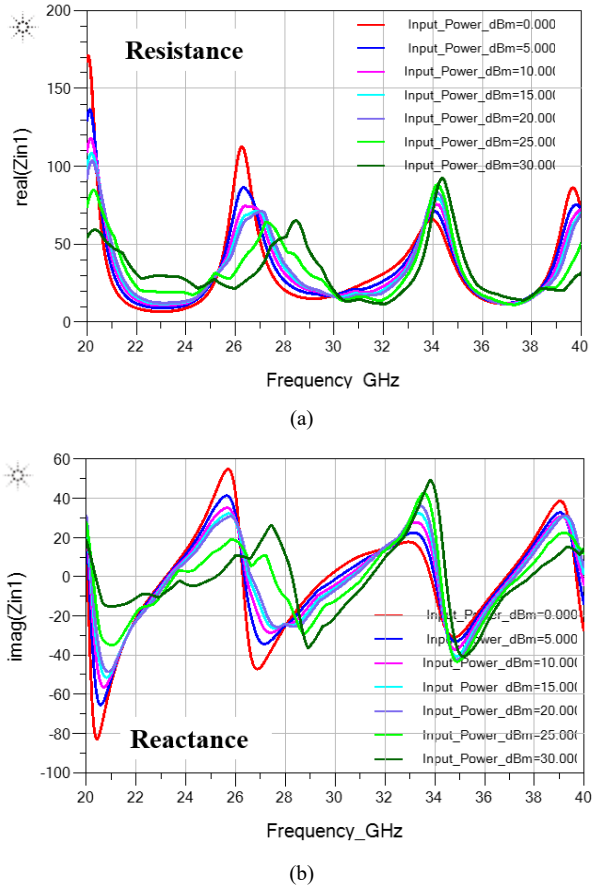

Fig. 8. (a) Resistance and (b) reactance of mmWave diode MA4E1317-based single diode rectifier at different powers from 0 to 30 dBm and frequency span from 20 to 40 GHz. The load impedance is 100 ohms.

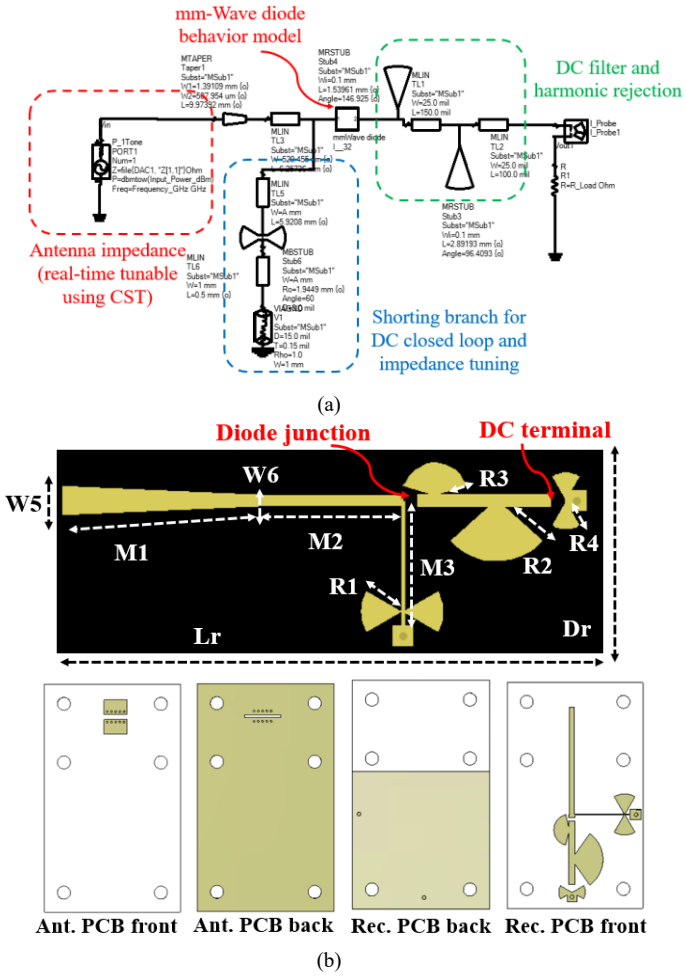

Fig. 9. (a) Schematic diagram of the co-designed wideband mmWave rectenna. (b) Layout of the proposed mmWave rectifier and PCB layer structure. W5 = 1.4 mm, W6 = 0.5 mm, M1 = 10 mm, M2 = 6.3 mm, M3 = 5.9 mm, R1 = 1.9 mm, R2 = 2.9 mm, R3=1.5 mm, R4 =1.3 mm, Lr = 35 mm, Dr = 16 mm.

diode model is particularly suitable for rectifier design for a large dynamic range in terms of power and frequency. As shown in Fig. 7, the diode mode jointly utilizes the SPICE parameter of MA4E1317 and parasitic elements that are determined by the *I−V, C−V*, and small signal S-parameters.

To analyze the performance of the MA4E1317 diode at the circuit level, we constructed a simple series diode circuit using ADS software, as illustrated in Fig. 7. We numerically swept the impedance *Z(f, P, L)* of the rectifier, considering a load of L = 100 ohms, as a function of frequency ranging from 20 GHz to 40 GHz, and as a function of input power ranging from 0 dBm to 30 dBm (representative power levels for wireless charging). The results are presented in Fig. 8.

The diode exhibits several resonances at approximately 26 GHz, 34 GHz, and 40 GHz. Both the real part (resistance) and the imaginary part (reactance) of the impedance are sensitive to changes in input power, with a variation range and frequency shift of around 15-20%. Notably, the impedance variation is much more pronounced compared to low-frequency diodes. These results serve as valuable reference data for determining the frequency dependence of the ME-dipole antenna impedance, as depicted in Fig. 6. By utilizing such impedance curves, we can achieve a co-designed conjugate matching across the wide frequency range of 20 GHz to 40 GHz.

C. *mmWave Rectifier Co-design*

The schematic diagram of the proposed rectifier is shown in Fig. 9(a), where the tunable antenna impedance is imported into ADS for the rectifier co-design. The co-design process was conducted in real-time, with the antenna impedance being updated immediately by optimizing the CST antenna structures based on the feedback information of the ADS rectifier efficiency and impedance matching performance. In this way, the ADS was utilized to tune the CST antenna impedance for achieving complete matching of the wideband rectenna.

Such a method has been reported in our previous papers [43, 44] as well as in some other papers [45, 46]. However, it is important to note that all these previous studies primarily focused on frequencies below 5 GHz. As the loss of SMD components and rectifying diodes significantly increases at mmWave frequencies, a new design method specifically suitable for mmWave rectenna co-design is necessary. Our work addresses this gap and presents a novel design method that caters to the unique challenges of mmWave frequencies, which has not been previously explored in the literature.

To model the mmWave rectifier, our main objective is to minimize the use of SMD components, high-frequency diodes,

and soldering. In our approach, a shunt circuit branch is positioned before the series-connected behavior model of the mmWave diode MA4E1317. Following the diode model, two DC filters (radial stubs) are connected to reject the higher order harmonics at 36 GHz and 48 GHz, respectively. This configuration forms a closed-circuit loop, consisting of the shunt branch, diode, DC filters, and load. By applying Kirchhoff's voltage law (KVL), voltage drops can be accounted for, ensuring the generation of a non-zero output voltage with minimal circuit components.

The overall design of the rectifier is kept simple, without the need for a dedicated impedance matching network. Instead, a taper line is employed to smoothly feed the antenna, facilitating the transmission of broadband impedance in the real part. It is important to note that while the shunt circuit branch primarily serves the purpose of a DC closed loop, its contribution to impedance tuning is limited due to its shunt inductance equivalence.

Once the antenna impedance is tuned by adjusting the ME-dipole parameters (as depicted in Fig. 3), the frequency and power-dependent impedance of the rectifier are updated accordingly to achieve optimal conjugate matching across the wide frequency range [43, 44]. Simultaneously, the rectifier topology undergoes updates to accommodate this dynamic co-design concept. The optimized rectifier topology is illustrated in Fig. 9(b), and the corresponding dimensions are provided in the captions. Notably, the overall rectifier design is nearly solderless. Only one diode junction and one DC terminal (for the chip resistor) require soldering, effectively minimizing the negative effects associated with multiple soldering points in conventional wideband impedance matching networks and SMD components.

Additionally, it is important to mention the presence of two via holes on the rectifier. One via hole is designated for the shunt circuit branch, while the other is for the ground connection of the DC terminal. These holes will be metallized with a gold coating during fabrication to minimize their impact on circuit performance. The utilization of double radial stubs for the mmWave rectifier via holes offers advantages in terms of low loss, high tolerance, and high precision during prototype fabrication [49]. Therefore, these stubs are employed to achieve the ultimate objective of realizing high-efficiency wideband mmWave rectennas with minimal insertion loss.

Compared to existing co-design strategies for low-frequency wideband rectennas, our method provides a unique guideline to effectively mitigate component losses at mmWave frequencies. It achieves this by transforming all necessary circuit components into a printed layout with low loss and high reliability. This approach allows for an elegant reduction in component losses, specifically tailored for the challenges of mmWave frequencies.

The rectifier topology in Fig. 9(b) will be printed on a single layer, double-sided high-frequency RT5880 substrate with a sheet thickness of 0.254 mm. The overall dimension is just $35 \times 16 \times 0.254\ mm^3$. An example of stacking the ME-dipole antenna on top of the rectifier is also shown in the figure where the rectifier and antenna share the same ground plane, which is

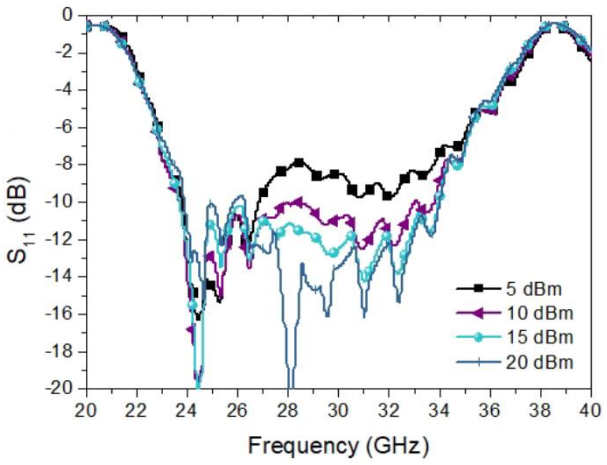

(a)

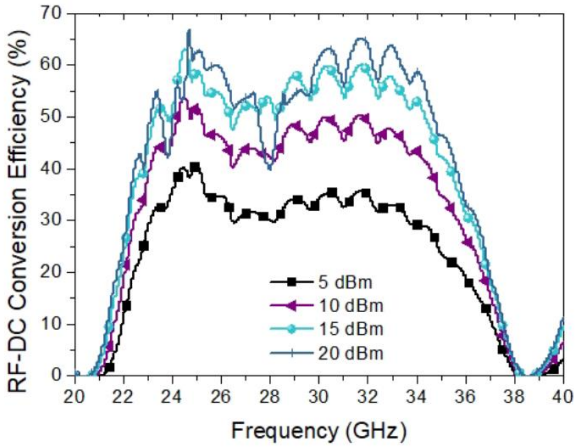

(b)

Fig. 10. (a) Reflection coefficient of the co-designed rectenna vs. frequency at three power levels. The reflection coefficient is calculated using the complex impedance of antenna and rectifiers. (b) RF-DC conversion efficiency of the proposed wideband mmWave rectenna vs. frequency at three power levels.

sandwiched in the middle. Having optimized the co-designed rectenna, the simulated S_{11} and RF-DC conversion of the proposed mmWave rectenna are depicted in Fig. 10(a) and (b). It is worth noting here that the calculation of S_{11} utilizes the complex impedance of the ME dipole antenna and rectifiers, rather than the conventional 50-ohm impedance. Our investigation into the frequency dependence within the range of 20 GHz to 40 GHz has revealed that the rectenna exhibits relatively good impedance matching over the 24 GHz to 34 GHz range. Moreover, we have achieved a conversion efficiency of up to 67% when the input power level is 20 dBm. The average conversion efficiency across the wide bandwidth is > 30%, 40%, 50% and 55% for input power levels at 5 dBm, 10 dBm, 15 dBm and 20 dBm respectively.

Please note the presented conversion efficiency is calculated using a load resistance of 100 ohms and using the formula below.

$$\eta_{RF-DC} = \frac{V_{DC}^2}{R_L \times P_{RF}} \quad (1)$$

where P_{RF} is the received RF power by the antenna, or in other words, the input RF power to the rectifier, V_{DC} is the output voltage and R_L = 100 ohms. In addition, the power dependence of the rectifier performance is analysed at three different frequencies (24 GHz, 29 GHz, 34 GHz) and shown in Fig. 11.

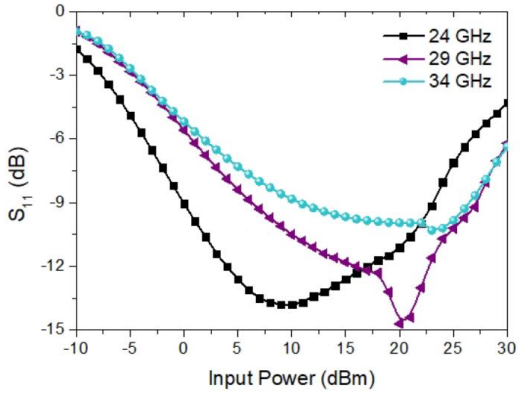

(a)

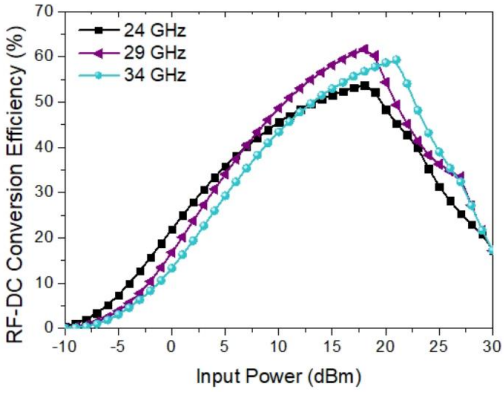

(b)

Fig. 11. (a) Reflection coefficient of the co-designed rectenna vs. power at three frequencies. (b) RF-DC conversion efficiency of the proposed wideband mmWave rectenna vs. power at three frequencies.

The optimal input power range for this rectenna is around 0 – 27 dBm in which the S_{11} is less than -9 dB for matching.

In terms of the power-dependent conversion efficiency, the proposed rectenna has a peak efficiency of around 50-65% at around 20 dBm power at different frequencies, and the efficiency nearly drops to 0 at the input power of -10 dBm. In summary, the proposed wideband rectenna can indeed perform well for a wide FBW of 34.5% (24 – 34 GHz) with RF-DC conversion efficiency above 50% for power > 15 dBm, and a rectifiable power range of 5 dBm – 27 dBm (efficiency around 30-60%).

IV. Fabrication and Measurement

The proposed rectenna was fabricated using high-precision laser PCB etching technology. The prototype is shown in Fig. 12(a), illustrating the front and back sides of the device. The ME dipole, which plays a crucial role in the rectenna, is highlighted within a 20 mm by 10 mm area. The backside of the ME dipole is fully metallized, except for a centralized slot for rectifier feeding. The rectifier itself was printed on a double-sided PCB, and its placement did not interfere with the overlapping region of the top ME dipole. In this region, the ground metal was removed to allow for feed line co-integration. The assembly of the entire rectenna was achieved without the need for soldering or gluing. Instead, 6 air holes were drilled along the PCB edges, and nylon screws were tightly fitted into these holes to secure the components, as depicted in Fig. 12(a).

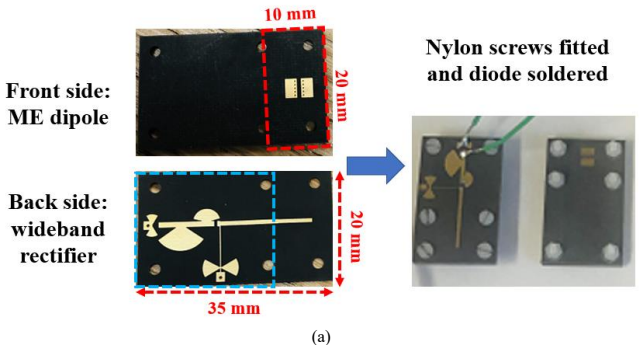

(a)

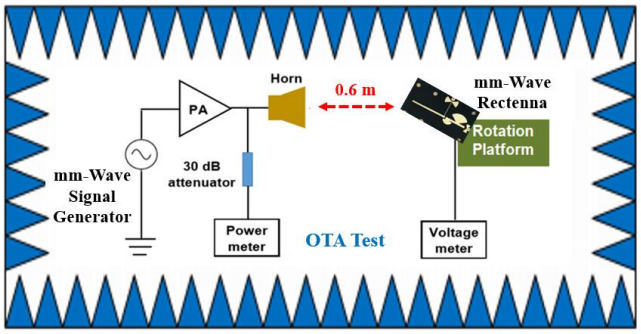

(b)

Fig. 12. (a) Fabricated prototype of the proposed mmWave rectenna. (b) Measurement setup for OTA test of the rectenna within an anechoic chamber.

To ensure the proper flow of DC current and maintain the rectifier's performance and load impedance, the DC wires were soldered after the rectifying diodes and DC pass filters. This configuration only permits the passage of DC current through the wires, without affecting the RF performance of the rectifier. During the measurement process, we compared the results obtained using both DC wires and DC probes and found that they yielded identical performance.

The measurement setup of the rectenna is shown in Fig. 12(b). Wideband mmWave signal generator N5183B was used to generate the signal from 20 to 40 GHz, which was then amplified by a 10 W MMIC wideband mmWave power amplifier QPA2640D manufactured by Qorvo. The signal was transmitted through high gain 18-40 GHz horn antenna HA40G, and was measured by using a power meter (spectrum analyzer) and a 30 dB attenuator and. The rectenna was tested over-the-air (OTA) at 0.6 m distance to the horn inside an anechoic chamber, where the broadside direction of the ME dipole was targeted toward the horn. The received power by the rectenna can be calculated using

$$P_r = P_t + G_t + G_r + 20\log_{10}\frac{\lambda}{4\pi D} \quad (2)$$

where P_r is the input RF power to the rectifier in dBm, P_t is the transmitting power of the horn in dBm, G_t is the realized gain of the horn in dBi, Gr is the realized gain of the proposed rectenna in dBi, λ is the wavelength of interest, and D is the distance (D = 0.6 m). Here the realized gain (ME dipole directivity × rectenna matching efficiency) of the rectenna was used, therefore might be not perfectly accurate. But such a method has shown good result consistency and accuracy in such integrated rectenna design in our previous work [43, 44] and other published papers [29, 31]. Indeed, validating conjugate matching experimentally is complex, as conventional methods

TABLE I
COMPARISON OF THE PROPOSED WIDEBAND MM-WAVE RECTENNA AND RELATED DESIGNS

Ref. (year)	Impedance bandwidth (GHz)	FBW*	Need impedance matching	Overall complexity	Overall dimension of the complete rectenna	Maximum conversion efficiency	Rectenna overall gain and half power beamwidth
[25] (2020)	20 – 26.5	28%	Yes	Medium	32.6 mm × 16 mm × 0.3 mm	12% at 10 dBm	~8 dBi and ~50 degrees (single antenna + rectifier)
[29] (2014)	23.5 – 25.2	6.9%	Yes	Complex	55 mm × 50 mm × 1.8 mm	40% at 20 dBm	~12.6 dBi and ~40 degrees (antenna array + rectifier)
[31] (2021)	34.5 – 35.5	3%	Yes	Complex	32 mm × 128 mm × 1 mm	60.9% at 19 dBm	~14.7 dBi and ~30 degrees (antenna array + rectifier)
This work (2022)	**24 – 34.5**	**36%**	**No**	**Simplest**	**35 mm × 20 mm × 1.9 mm**	**67% at 20 dBm**	~8 dBi and ~90 degrees (single antenna + rectifier)

*FBW: Factional Bandwidth

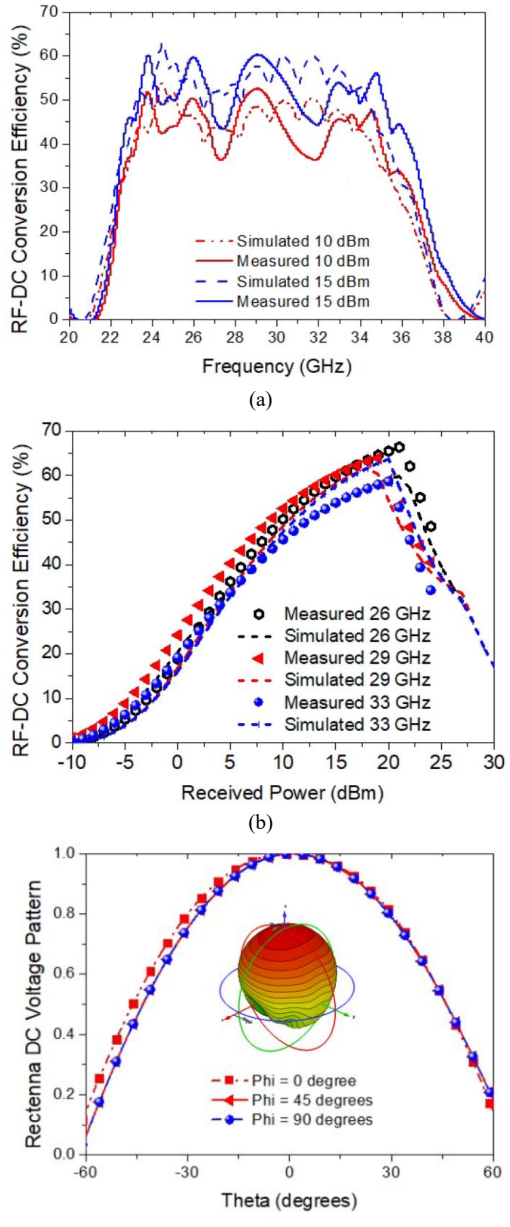

Fig. 13. Experimental results of the proposed rectenna for (a) RF-DC conversion efficiency vs. frequency. (b) RF-DC conversion efficiency vs. power and (c) normalized DC voltage pattern of the rectenna at different cutting angles.

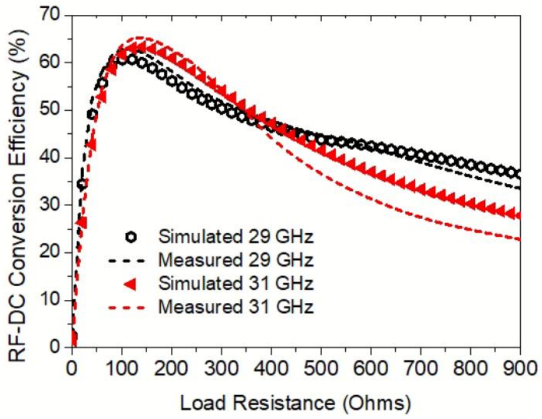

Fig. 14. Comparison between simulated and measured RF-DC conversion efficiency vs. load resistance. The input power is fixed at 15 dBm during the experiment.

fall short. In our experimental setup, both antenna and rectifier underwent testing, assessing S-parameters with 50-ohm SMA connectors. This method gauges impedance on the Smith Chart, scrutinizing fabrication accuracy. We cross-validated simulation outcomes via 50-ohm SMAs, accounting for fabrication and diode model uncertainties. Although direct matching efficiency testing is challenging, separate experiments authenticate antenna and rectifier impedance, enabling optimized consistency. By adjusting the transmitting power, the received power can be maintained at a constant level over the wide frequency range. A comparison between the simulated and measured frequency-dependence of RF-DC conversion efficiency is depicted in Fig. 13 (a). The results are compared at 10 dBm and 15 dBm received power levels respectively, which show that the proposed rectenna can indeed realize very high conversion efficiency over the frequency band of interest. Moreover, the power dependence of the conversion efficiency is compared at 26, 29, and 33 GHz respectively (see Fig. 13(b)). The consistency between simulated and measured results is generally good, but we have just measured up to the power level of 24 dBm, due to the limits of saturation power (< 10 W) of the mmWave power amplifier.

Furthermore, to assess the performance of the rectenna, we placed it on a rotational platform inside the chamber. The received DC voltage was recorded at different Theta and Phi angles, with the antenna broadside as the reference. The

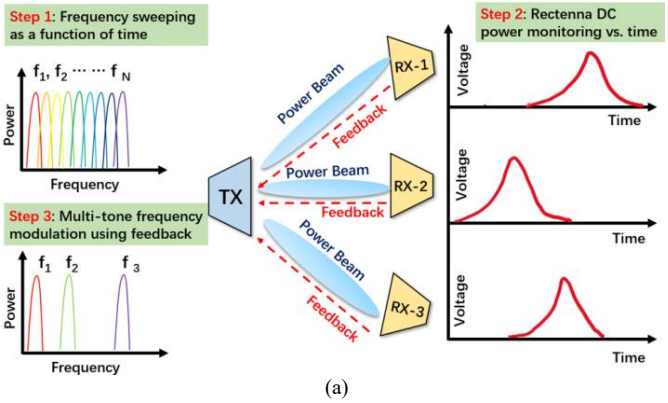

(a)

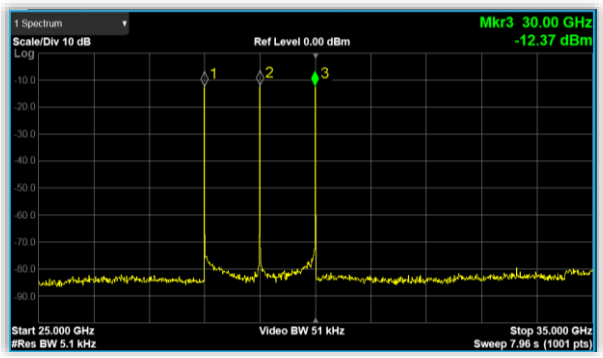

(b)

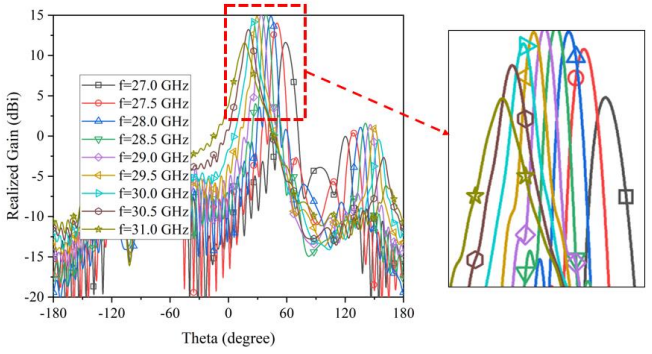

(c)

Fig. 15. (a) Proposed concept for multi-node wireless charging and tracking using the proposed WPT system. (b) Example of the multi-tone spectrum for mmWave modulation. (c) Beam scanning radiation pattern of the proposed LWA prototype [51].

normalized DC voltage pattern, obtained with a received power of 15 dBm and a maximum DC voltage of 1.42 V, is shown in Fig. 13 (c). The pattern demonstrates that the proposed rectenna exhibits a relatively wide beamwidth, spanning over 90 degrees. It is important to note that the DC voltage pattern of the rectenna may slightly differ from the ME-dipole radiation pattern due to the nonlinear rectifier and circuit loads [50]. To explore the impact of load resistance, we measured the proposed rectenna at a fixed input power of 15 dBm while varying the load resistance from 10 to 900 ohms. The results are presented in Fig. 15. It was observed that the peak efficiency occurred at a load resistance of 100 ohms, and the optimal load range for achieving an efficiency greater than 50% was approximately between 50 and 350 ohms. The validity of this load range was verified at two different frequencies, specifically 29 GHz and 31 GHz.

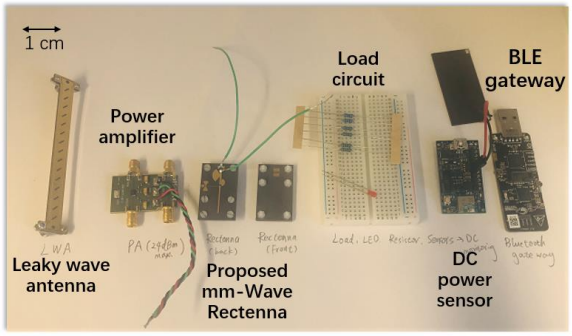

(a)

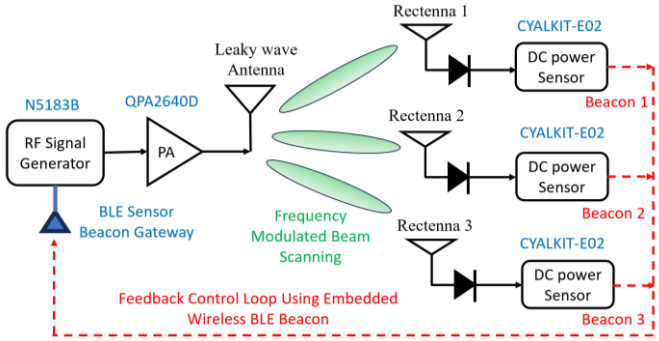

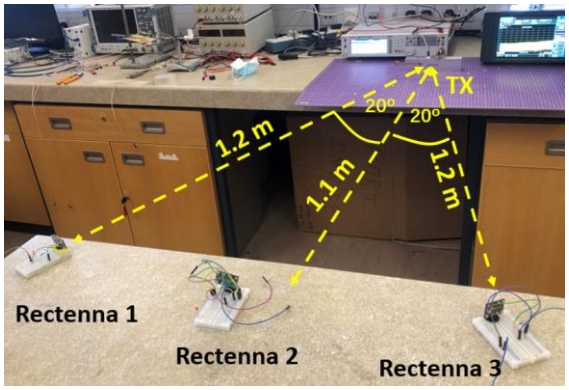

(b)

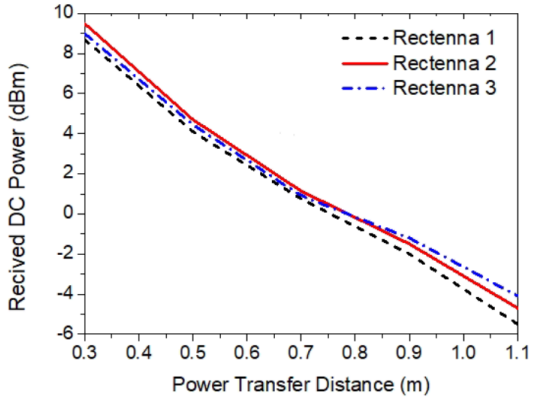

(c)

Fig. 16. (a) Prototypes and assembly for the proposed WPT system. (b) Example picture and system layout for wireless powering three rectenna nodes with feedback loop control. (c) Receiving rectenna node DC power vs. distance for transmitting EIRP of 55 dBm.

The proposed rectenna has been compared with state-of-the-art mmWave rectennas in terms of either wideband capability or high efficiency (see Table I). The comparison highlights the

unique features and advantages of our design. The comparison clearly demonstrates that our work achieves a significant enhancement in RF-DC conversion efficiency across a wide mmWave spectrum. This improvement is attributed to the co-designed structure, which enables lossless impedance matching and minimizes the negative effects of soldering on circuit performance. Compared to a single wideband antenna-based rectenna design [25], our efficiency is 40% higher, thanks to the utilization of a low-loss substrate and a novel integration method. Additionally, our design offers a broader beamwidth due to the wide-beam nature of the ME dipole. When compared to antenna array-based designs [29, 31], our design excels in terms of reduced physical size while maintaining high efficiency. In summary, our design showcases compactness, wide beamwidth, and commendable gain.

V. Multi-node Charging and Tracking

Unlike traditional radar (RDA) and phased array radar (TR) technologies, the wireless power transmitter based on leaky wave antenna (LWA) does not require complex antenna arrays, phase shifters, signal mixers, or active semiconductor switches. Instead, beamforming is achieved through software-controlled frequency modulation. This approach offers a simplified node tracking mechanism. To perform node tracking, the transmitter sweeps the frequency of the transmitting (TX) signal at a known rate over a defined time period. Concurrently, the DC power received from the RX rectenna node is continuously monitored in real-time, synchronized with the transmitter's frequency sweeping. When the peak DC output is detected, the receiver sends a beacon signal back to the transmitter, indicating the optimal time instance for beamforming at a specific TX signal frequency. This enables precise localization of the optimal frequency for beamforming.

Furthermore, our design allows for multi-target moving node tracking by utilizing multitone frequency modulation and sweeping, as illustrated in Fig. 15(a). The leaky wave antenna, as depicted in Fig. 15, exhibits unique beam shapes that vary with its operating frequency. This results in a scanning beam characteristic, offering a distinct advantage over conventional phased array scanning methods. In conventional approaches, beam scanning is achieved by manipulating the phase of antenna elements using phase shifters while keeping the frequency constant. In our work, we can achieve beam scanning simply by changing the input signal's frequency, which can be easily controlled through software using the signal generator.

Here we show an example of charging 3 different nodes simultaneously. The waveform for the frequency modulation is given in Fig. 15(b) which shows a three-tone CW signal at 28, 29, and 30 GHz respectively. The frequency tones could either be controlled using a time-switching fashion, or be excited at the same time, dependent on the number of receiving nodes and total TX power. A leaky-wave antenna prototype covering 27 – 31 GHz was employed to transmit the signal, where the frequency-dependent beam-scanning patterns of the LWA are shown in Fig. 15(c). It can be seen that the LWA could realize a 50-degree beam scanning range over 27 – 31 GHz, where the radiating angles for 28, 29, and 30 GHz are around Theta = 15, 30, and 45 degrees respectively [51]. In this work, the scanning range for a 1 dB gain drop spans from 23.5 to 50 degrees (with a frequency range of 27.5 to 30.2 GHz), while the 3 dB gain scanning range extends from 17 to 58.5 degrees (across a frequency range of 27 to 30.9 GHz).

The experimental system of the proposed mmWave multi-node charging and tracking is depicted in Fig. 16(a), which consists of prototypes for LWA, PA, proposed rectennas, load, node DC sensor, and BLE gateway for feedback control. The DC sensor was developed using a low-cost programmable sensor platform (CYALKIT-E02 BLE Sensor Beacon), which has been reported in our previous work [52]. The rectenna DC peak vs. time instance could be transmitted to the gateway and to identify the optimal frequency over the scanning frequency for TX. The scanning rate was 100 MHz per 500 μs over 28 – 30 GHz, configured within the signal source. An example of the 3-node simultaneous charging scenario is depicted in Fig. 16(b), where rectenna nodes 1, 2, and 3 were positioned at a 1-meter distance from the LWA transmitter. These rectennas were situated within the far-field beam angles of 15, 30, and 45 degrees. Within this range, bean scanning gain reduction is minimal—less than 1 dB, as evidenced by Fig. 15(c). Unlike standard antenna arrays, the coupling dynamics of rectenna arrays are distinct, as RF signals are rectified into DC under optimal matching conditions. This underscores the adequacy of a half-wavelength separation for rectenna array spacing. The EIRP was set at 55 dBm. By harnessing the multi-tone spectrum depicted in Fig. 15(b), the 3 receiving nodes can be efficiently powered wirelessly. The measured DC power output from the three nodes, plotted against the power transfer distance, is illustrated in Fig. 16(c). It can be seen that rectenna 2 has a bit higher power compared to rectennas 1 and 3. This was probably due to the slight gain drop of the LWA at 28 and 30 GHz, compared to its highest gain at 29 GHz (around 15 dBi).

We would like to emphasize that the proposed WPT system is preliminary research, and it is the first time to showcase multi-target charging using mmWave power. There is still plenty of room for further investigations, for example, 1) the adaptive DC control for PA to mitigate the gain diversity of different frequencies; 2) fast feedback control for moving targets and 3) a more effective LWA transmitter with higher gain, smaller size and wide scanning angles over limited spectrums. In comparison to our previous conference contribution in [53], which provided a brief introduction to the overall system structure and emphasized the significance of wideband mmWave rectenna design, this paper substantially delves into the technical intricacies of mmWave rectenna co-design. It comprehensively covers various aspects, such as diode modeling, antenna impedance optimization, rectifier co-simulation, and the underlying physics behind all simulation and experimental results. Furthermore, this paper incorporates an extensive set of experimental results to demonstrate the feasibility of mmWave WPT and to quantify the performance of the novel mmWave wideband rectenna.

VI. Conclusion

In this paper, we have presentted a co-design strategy for mmWave rectennas, enabling them to cover a wide frequency bandwidth (>36%) while achieving high RF-DC conversion efficiency (>50%, up to 67%). Our approach involves

combining a magnetoelectric (ME) dipole with high-frequency MA4E1317 diodes, allowing for efficient antenna-to-rectifier impedance matching without the need for transmission line components at the circuit level. The proposed rectenna offers several advantages, including wide bandwidth, wide beam width, and improved efficiency at mmWave frequencies. Furthermore, we demonstrate the practical application of the proposed rectenna in a multi-node simultaneous wireless charging system. Our preliminary results showcase the feasibility of passive beamforming using multi-tone frequency modulated leaky wave antenna (LWA) transmitters to power three wideband rectenna nodes.

Moving forward, our future work will focus on feedback control and moving target tracking using the proposed rectenna and wireless power transfer (WPT) system. These advancements hold great potential for enhancing the capabilities and efficiency of mmWave beamformed wireless charging. As the first demonstration of passive mmWave beamformed wireless charging, our work has significant implications for both the academic and commercial wireless power research community.

REFERENCES

[1] B. Strassner and K. Chang, "Microwave Power Transmission: Historical Milestones and System Components," *Proc. IEEE*, vol. 101, no. 6, pp. 1379-1396, June 2013.

[2] G. A. Covic and J. T. Boys, "Inductive Power Transfer," *Proc. IEEE*, vol. 101, no. 6, pp. 1276-1289, June 2013。

[3] J. S. Ho, S. Kim and A. S. Y. Poon, "Midfield Wireless Powering for Implantable Systems," *Proc. IEEE*, vol. 101, no. 6, pp. 1369-1378, June 2013.

[4] A. Costanzo *et al*., "Electromagnetic Energy Harvesting and Wireless Power Transmission: A Unified Approach," *Proc. IEEE*, vol. 102, no. 11, pp. 1692-1711, Nov. 2014.

[5] C. Song *et al*., "Advances in Wirelessly Powered Backscatter Communications: From Antenna/RF Circuitry Design to Printed Flexible Electronics," *Proc. IEEE*, vol. 110, no. 1, pp. 171-192, Jan. 2022.

[6] S. Assawaworrarit, X. Yu, and S. Fan, "Robust wireless power transfer using a nonlinear parity–time-symmetric circuit," *Nature*, vol. 546, pp. 387–390, Jun. 2017.

[7] S. Y. Hui, "Planar Wireless Charging Technology for Portable Electronic Products and Qi," *Proc. IEEE*, vol. 101, no. 6, pp. 1290-1301, June 2013.

[8] A. Kurs, A. Karalis, R. Moffatt, J. D. Joannopoulos, P. Fisher, and M. Soljacic, "Wireless power transfer via strongly coupled magnetic resonances," *Science,* vol. 317, pp. 83–86, Jul. 6, 2007.

[9] A. P. Sample, D. T. Meyer, and J. R. Smith, "Analysis, experimental results, and range adaptation of magnetically coupled resonators for wireless power transfer," *IEEE Trans. Ind. Electron*., vol. 58, no. 2, pp. 544–554, Feb. 2011.

[10] P. Jaffe and J. McSpadden, "Energy Conversion and Transmission Modules for Space Solar Power," *Proc. IEEE*, vol. 101, no. 6, pp. 1424-1437, June 2013.

[11] S. Kawasaki, "Microwave WPT to a rover using active integrated phased array antennas," *Proceedings of the 5th European Conference on Antennas and Propagation (EUCAP)*, 2011, pp. 3909-3912.

[12] J. H. Park, D. I. Kim and K. W. Choi, "Analysis and Experiment on Multi-Antenna-to-Multi-Antenna RF Wireless Power Transfer," *IEEE Access*, vol. 9, pp. 2018-2031, 2021.

[13] D. Masotti, A. Costanzo, M. Del Prete and V. Rizzoli, "Time-Modulation of Linear Arrays for Real-Time Reconfigurable Wireless Power Transmission," *IEEE Trans. Microw. Theory Tech.*, vol. 64, no. 2, pp. 331-342, Feb. 2016.

[14] B. Yang, X. Chen, J. Chu, T. Mitani and N. Shinohara, "A 5.8-GHz Phased Array System Using Power-Variable Phase-Controlled Magnetrons for Wireless Power Transfer," *IEEE Trans. Microw. Theory Tech.*, vol. 68, no. 11, pp. 4951-4959, Nov. 2020.

[15] H. -Y. Zhang, F. -S. Zhang, F. Zhang, F. -K. Sun and G. -J. Xie, "High-Power Array Antenna Based on Phase-Adjustable Array Element for Wireless Power Transmission," *IEEE Antennas Wireless Propag. Lett.*, vol. 16, pp. 2249-2253, 2017.

[16] J. Han *et al*., "Adaptively Smart Wireless Power Transfer Using 2-Bit Programmable Metasurface," *IEEE Trans. Ind. Electron*., vol. 69, no. 8, pp. 8524-8534, Aug. 2022.

[17] S. Yu, H. Liu and L. Li, "Design of Near-Field Focused Metasurface for High-Efficient Wireless Power Transfer With Multifocus Characteristics," *IEEE Trans. Ind. Electron.,* vol. 66, no. 5, pp. 3993-4002, May 2019.

[18] R. González Ayestarán, G. León, M. R. Pino and P. Nepa, "Wireless Power Transfer Through Simultaneous Near-Field Focusing and Far-Field Synthesis," *IEEE Trans. Antennas Propag.*, vol. 67, no. 8, pp. 5623-5633, Aug. 2019.

[19] Y. -Q. Yang, H. Wang and Y. -X. Guo, "A Time-Modulated Array With Digitally Preprocessed Rectangular Pulses for Wireless Power Transmission," *IEEE Trans. Antennas Propag.*, vol. 68, no. 4, pp. 3283-3288, April 2020.

[20] P. D. Hilario Re, S. K. Podilchak, S. A. Rotenberg, G. Goussetis and J. Lee, "Circularly Polarized Retrodirective Antenna Array for Wireless Power Transmission," *IEEE Trans. Antennas Propag.*, vol. 68, no. 4, pp. 2743-2752, April 2020.

[21] H. S. Park and S. K. Hong, "Investigation of Time-Reversal Based Far-Field Wireless Power Transfer From Antenna Array in a Complex Environment," *IEEE Access*, vol. 8, pp. 66517-66528, 2020.

[22] Z. -H. Cheng *et al*., "Selectively Powering Multiple Small-Size Devices Spaced at Diffraction Limited Distance With Point-Focused Electromagnetic Waves," *IEEE Trans. Ind. Electron.*, vol. 69, no. 12, pp. 13696-13705, Dec. 2022.

[23] S. Mizojiri and K. Shimamura, "Wireless power transfer via subterahertz-wave," *Appl. Sci*., vol. 8, no. 12, p. 2653, Dec. 2018.

[24] D. Surender, M. A. Halimi, T. Khan, F. A. Talukdar, Nasimuddin and S. R. Rengarajan, "5G/Millimeter-Wave Rectenna Systems for Radio-Frequency Energy Harvesting/Wireless Power Transmission Applications: An overview," *IEEE Antennas Propagat. Mag.*, vol. 65, no. 3, pp. 57-76, June 2023.

[25] M. Wagih, G. S. Hilton, A. S. Weddell and S. Beeby, "Broadband Millimeter-Wave Textile-Based Flexible Rectenna for Wearable Energy Harvesting," *IEEE Trans. Microw. Theory Tech.,* vol. 68, no. 11, pp. 4960-4972, Nov. 2020.

[26] A. Eid, J. G. D. Hester, and M. M. Tentzeris, "5G as a wireless power grid," *Sci. Rep.*, vol. 11, no. 1, pp. 1–9, Dec. 2021.

[27] M. Bozzi, A. Georgiadis, and K. Wu, "High-efficiency microstrip rectenna for microwave power transmission at Ka band with low cost," *IET Microw. Antennas Propag*., vol. 10 no. 15, pp. 1648–1655, 2016.

[28] A. Takacs, H. Aubert, S. Fredon, L. Despoisse, and H. Blondeaux, "Microwave power harvesting for satellite health monitoring," *IEEE Trans. Microw. Theory Techn.*, vol. 62, no. 4, pp. 1090–1098, Feb. 2014.

[29] S. Ladan, A. B. Guntupalli and K. Wu, "A High-Efficiency 24 GHz Rectenna Development Towards Millimeter-Wave Energy Harvesting and Wireless Power Transmission," *IEEE Trans. Circuits Syst. I, Reg. Papers*, vol. 61, no. 12, pp. 3358-3366, Dec. 2014.

[30] S. Ladan and K. Wu, "Nonlinear Modeling and Harmonic Recycling of Millimeter-Wave Rectifier Circuit," *IEEE Trans. Microw. Theory Tech.,* vol. 63, no. 3, pp. 937-944, March 2015.

[31] Y. Wang, X. -X. Yang, G. -N. Tan and S. Gao, "Study on Millimeter-Wave SIW Rectenna and Arrays With High Conversion Efficiency," *IEEE Trans. Antennas Propag.*, vol. 69, no. 9, pp. 5503-5511, Sept. 2021.

[32] Y. Huang, *Antennas: From Theory to Practice*. Chichester, 2nd Ed., U.K.: Wiley, 2021.

[33] M. Wagih, A. S. Weddell and S. Beeby, "Millimeter-Wave Power Harvesting: A Review," *IEEE Open J. Antennas Propag*, vol. 1, pp. 560-578, 2020.

[34] A. A. Oliner and D. R. Jackson, *"Leaky-wave antennas"* in Antenna Engineering Handbook, New York, NY, USA:McGraw-Hill, 2007.

[35] X. Li, J. Wang, G. Goussetis and L. Wang, "Circularly Polarized High Gain Leaky-Wave Antenna for CubeSat Communication," *IEEE Trans. Antennas Propag.*, vol. 70, no. 9, pp. 7612-7624, Sept. 2022.

[36] Q. Xue, S. W. Liao and J. H. Xu, "A Differentially-Driven Dual-Polarized Magneto-Electric Dipole Antenna," *IEEE Trans. Antennas Propag.*, vol. 61, no. 1, pp. 425-430, Jan. 2013.

[37] J. Wang, Y. Li, L. Ge, J. Wang and K. -M. Luk, "A 60 GHz Horizontally Polarized Magnetoelectric Dipole Antenna Array With 2-D Multibeam Endfire Radiation," *IEEE Trans. Antennas Propag.*, vol. 65, no. 11, pp. 5837-5845, Nov. 2017.

[38] J. Zeng and K. -M. Luk, "Wideband Millimeter-Wave End-Fire Magnetoelectric Dipole Antenna With Microstrip-Line Feed," *IEEE Trans. Antennas Propag.*, vol. 68, no. 4, pp. 2658-2665, April 2020.

[39] X. Dai, G. -B. Wu and K. -M. Luk, "A Wideband Circularly Polarized Transmitarray Antenna for Millimeter-Wave Applications," *IEEE Trans. Antennas Propag.*, vol. 71, no. 2, pp. 1889-1894, Feb. 2023.

[40] C. Song, E. L. Bennett, J. Xiao and Y. Huang, "Multimode Hybrid Antennas Using Liquid Dielectric Resonator and Magneto-Electric Dipole," *IEEE Trans. Antennas Propag.*, vol. 69, no. 6, pp. 3132-3143, June 2021

[41] H. W. Lai and H. Wong, "Substrate Integrated Magneto-Electric Dipole Antenna for 5G Wi-Fi," *IEEE Trans. Antennas Propag*., vol. 63, no. 2, pp. 870-874, Feb. 2015.

[42] K. Kang, Y. Shi and C. -H. Liang, "Substrate Integrated Magneto–Electric Dipole for UWB Application," *IEEE Antennas Wirel. Propag. Lett.*, vol. 16, pp. 948-951, 2017

[43] C. Song *et al*., "Matching Network Elimination in Broadband Rectennas for High-Efficiency Wireless Power Transfer and Energy Harvesting," *IEEE Trans. Ind. Electron*., vol. 64, no. 5, pp. 3950-3961, May 2017.

[44] C. Song, Y. Huang, P. Carter, J. Zhou, S. D. Joseph and G. Li, "Novel Compact and Broadband Frequency-Selectable Rectennas for a Wide Input-Power and Load Impedance Range," *IEEE Trans. Antennas Propag.*, vol. 66, no. 7, pp. 3306-3316, July 2018.

[45] A. Lopez-Yela and D. Segovia-Vargas, "A triple-band bow-tie rectenna for RF energy harvesting without matching network," *2017 IEEE Wireless Power Transfer Conference (WPTC)*, Taipei, Taiwan, 2017, pp. 1-4.

[46] T. S. Almoneef, "Design of a Rectenna Array Without a Matching Network," *IEEE Access*, vol. 8, pp. 109071-109079, 2020.

[47] S. -P. Gao, W. Hu, H. Zhang and Y. Guo, "Millimeter-Wave Rectifiers Using Proprietary Schottky Diodes: Diode Modeling and Rectifier Analysis," *2022 Wireless Power Week (WPW)*, 2022, pp. 180-184.

[48] Q. Chen, X. Chen, H. Cai and F. Chen, "A Waveguide-Fed 35-GHz Rectifier With High Conversion Efficiency," *IEEE Microw. Wireless Compon. Lett.*, vol. 30, no. 3, pp. 296-299, March 2020.

[49] S. Ladan, S. Hemour and K. Wu, "A millimeter-wave wideband microstrip RF and DC grounding," *2012 42nd European Microwave Conference*, 2012, pp. 13-16.

[50] T. Q. V. Hoang, E. Séguenot, F. Ferrero, J. -L. Dubard, P. Brachat and J. -L. Desvilles, "3D Voltage Pattern Measurement of a 2.45 GHz Rectenna," *IEEE Trans. Antennas Propag.*, vol. 61, no. 6, pp. 3354-3356, June 2013.

[51] X. Li, L. Wang, J. Wang and G. Goussetis, "Conformal High Gain Aperture Antenna Based on Leaky-Wave Array for CubeSat Communication," *2020 International Symposium on Antennas and Propagation (ISAP*), 2021, pp. 499-500.

[52] C. Song, P. Lu and S. Shen, "Highly Efficient Omnidirectional Integrated Multiband Wireless Energy Harvesters for Compact Sensor Nodes of Internet-of-Things," *IEEE Trans. Ind. Electron*., vol. 68, no. 9, pp. 8128-8140, Sept. 2021.

[53] C. Song, L. Wang, Z. Chen, G. Goussetis, G. A. E. Vandenbosch and Y. Huang, "Wideband mmWave Wireless Power Transfer: Theory, Design and Experiments," *2023 17th European Conference on Antennas and Propagation (EuCAP)*, Florence, Italy, 2023.

Chaoyun Song (Senior Member, IEEE) received BEng. MSc and PhD degrees in electrical engineering and electronics from The University of Liverpool (UoL), Liverpool, UK, in 2012, 2013 and 2017, respectively.

He is currently an Associate Professor (Senior Lecturer) with the Department of Engineering, King's College London, London, UK. Prior to this, he was an Assistant Professor with the School of Engineering and Physical Sciences (EPS), Heriot-Watt University, Edinburgh, Scotland, UK. He has published more than 110 papers (including 45 IEEE transactions) in peer-reviewed journals and conference proceedings. His current research interests include wireless energy harvesting and power transfer, rectifying antennas (rectennas), flexible and stretchable electronics, metamaterials and meta-surface, and low-power sensors.

Dr. Song has been the recipient of numerous international awards, including the IEEE AP-S Young Professional Ambassador 2023, IEEE AP-S Raj Mittra Travel Grant 2023, EuCAP 2023 Best Antenna Paper Award, IET Innovation Award in 2018, and BAE Systems Chairman's Award in 2017. Additionally, Dr. Song has served as a session chair and/or TPC member for various conferences, including EuCAP2018, IEEE AP-S Symposium 2021, IEEE VTC2022-fall, EuCAP2023, IEEE AP-S Symposium 2023 and EuCAP2024. He has consistently contributed as a reviewer for esteemed journals such as Nature Electronics, Nature Communications, Advanced Materials, Advanced Functional Materials, and Nano Energy, in addition to reviewing for over fifteen IEEE Transactions. He is a Top-200 reviewer for IEEE Transactions on Antenna and Propagation (2021-2023). Dr. Song has also taken on the role of Guest Editor for prestigious publications including IEEE Open Journal on Antennas and Propagation, IET Electronic Letters, Micromachines, and Wireless Communications and Mobile Computing and an Associate Editor for Frontiers in Communications and Networks.

Lei Wang (Senior Member, IEEE) received the Ph.D. degree in electromagnetic field and microwave technology from the Southeast University, Nanjing, China in 2015. From November 2017 to February 2020, he was an Alexander von Humboldt scholar in the Institute of Electromagnetic Theory of Hamburg University of Technology (TUHH) in Hamburg, Germany. From March 2020 to present, he is an Assistant Professor in the Institute of Signals, Sensors and Systems of Heriot-Watt University in Edinburgh, United Kingdom. His research includes the antenna theory and applications, active electronically scanning arrays, integrated antennas and arrays, substrate-integrated waveguide antennas, leaky-wave antennas, and wireless propagations.

He was awarded the Chinese National Scholarship for PhD Candidates in 2014 and was granted the Swiss Government Excellence Scholarship to conduct research at EPFL in 2014 too. He was also granted by the Alexander von Humboldt Research Foundation to take research at TUHH in 2016. Moreover, he received the Best Poster Award in 2018 IEEE International Workshop on Antenna Technology (iWAT) and the Best Paper Award in the 5th International Conference on the UK-China Emerging Technologies (UCET2020).

Ping Lu (Member, IEEE) received the B.S. degree in electrical engineering and automation from Southwest Jiaotong University, Chengdu, China, in 2012, and the Ph.D. degree in radio physics from the University of Electronic Science and Technology, Chengdu, in 2018.,From 2015 to 2017, she was a Joint Ph.D. Student Scholar with the Laboratoire Ampére, École Centrale de Lyon, INSA de Lyon, Université Claude Bernard de Lyon, Villeurbanne, France. She is currently an Associate Professor with the School of Electronics and Information Engineering, Sichuan University, Chengdu. Her current research interests include rectenna, non-diffraction beams, and wireless power transmission.

Cheng Zhang was born in Henan, China. He received the M.S. degree in material science and technology from Wuhan University of Technology, Wuhan, China, in 2015, and the Ph.D degree at the State Key Laboratory of Millimeter Waves, Department of Radio Engineering, Southeast University, Nanjing, in 2019. He is currently a Professor in Shanghai Institute of Optics and Fine Mechanics, Chinese Academy of Sciences, Shanghai 201800, China. His current research interests are EM energy harvesting, stealth metamaterial/metasurface and multi-physical manipulation. He has authored or co-authored more than fifty publications (including six highly cited papers), with citation over 1500 times.

He was a recipient of the 2020 CHINA TOP CITED PAPER AWARD from IOP Publishing and Top Articles in Device Physics for Applied Physics Letters (two papers). He received the Honor mention award for best student paper contest in 2018 IEEE International Workshop on Antenna Technology (iWAT) and the Appreciation award of invited talk in 2018 IEEE International Conference on Computational Electromagnetics (ICCEM).

Zhensheng Chen received the B.Eng. and M.Sc. degrees in communication engineering from Lanzhou University, Lanzhou, China, in 2015 and 2018, respectively. He is currently pursuing the Ph.D. degree with KU Leuven, Leuven, Belgium.,He joined Heriot-Watt University, Edinburgh, U.K., as a Visiting Ph.D. Researcher, in April 2022. His current research interests include wearable antennas, rectifying antennas, wireless power transfer (WPT), and RF energy harvesting (EH).

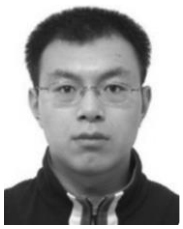

Xuezhi Zheng (Member, IEEE) received the M.S. degree in electrical engineering and the Ph.D. degree (summa cum laude) from KU Leuven, Leuven, Belgium, in 2010 and 2014, respectively.,From 2020 to 2021, he was a Visiting Scholar with the Nanophotonics Centre, Cavendish Laboratory, University of Cambridge, Cambridge, U.K. Since 2014, he has been a Post-Doctoral Researcher with the ESAT-WaveCore Group, KU Leuven. He is currently a Visiting Scholar with the Center for Polariton-Driven Light–Matter Interaction (POLIMA), Southern Denmark University, Odense, Denmark. His current research interests include the modeling of the interaction of electromagnetic (EM) waves with nanoscopic structures.

Yejun He (Senior Member, IEEE) received the Ph.D. degree in information and communication engineering from the Huazhong University of Science and Technology (HUST), Wuhan, China, in 2005. From 2005 to 2006, he was a Research Associate with the Department of Electronic and Information Engineering, The Hong Kong Polytechnic University, Hong Kong. From 2006 to 2007, he was a Research Associate with the Department of Electronic Engineering, Faculty of Engineering, The Chinese University of Hong Kong, Hong Kong. In 2012, he was a Visiting Professor with the Department of Electrical and Computer Engineering, University of Waterloo, Waterloo, ON, Canada. From 2013 to 2015, he was an Advanced Visiting Scholar (Visiting Professor) with the School of Electrical and Computer Engineering, Georgia Institute of Technology, Atlanta, GA, USA. Since 2011, he has been a Full Professor with the College of Electronics and Information Engineering, Shenzhen University, Shenzhen, China, where he is the Director of the Guangdong Engineering Research Center of Base Station Antennas and Propagation, Shenzhen, and the Director of the Shenzhen Key Laboratory of Antennas and Propagation, Shenzhen. He was selected as Pengcheng Scholar Distinguished Professor, Shenzhen, and a Minjiang Scholar Chair Professor of Fujian, China, in 2020 and 2022, respectively. He has authored or coauthored over 260 research papers and seven books, and holds about 20 patents. His research interests include wireless communications, antennas, and radio frequency. Dr. He is a Fellow of IET and a Senior Member of the China Institute of Communications and the China Institute of Electronics. He was a recipient of the Shenzhen Overseas High-Caliber Personnel Level B ("Peacock Plan Award" B) and Shenzhen High-Level Professional Talent (Local Leading Talent). He received the Shenzhen Science and Technology Progress Award in 2017 and the Guangdong Provincial Science and Technology Progress Award for two times in 2018 and 2023. He is currently the Chair of the IEEE Antennas and Propagation Society-Shenzhen Chapter and obtained the 2022 IEEE APS Outstanding Chapter Award. He has served as a Reviewer for various journals, such as the IEEE TRANSACTIONS ON VEHICULAR TECHNOLOGY, the IEEE TRANSACTIONS ON COMMUNICATIONS, the IEEE TRANSACTIONS ON INDUSTRIAL ELECTRONICS, the IEEE TRANSACTIONS ON ANTENNAS AND PROPAGATION, the IEEE WIRELESS COMMUNICATIONS, the IEEE COMMUNICATIONS LETTERS, the International Journal of Communication Systems, Wireless Communications and Mobile Computing, and Wireless Personal Communications. He has also served as a Technical Program Committee Member or a Session Chair for various conferences, including the IEEE Global Telecommunications Conference (GLOBECOM), the IEEE International Conference on Communications (ICC), the IEEE Wireless Communication Networking Conference (WCNC), APCAP, EUCAP, UCMMT, and the IEEE Vehicular Technology Conference (VTC). He served as the TPC Chair for IEEE ComComAp 2021, the General Chair for IEEE ComComAp 2019, the TPC Co-Chair for WOCC 2023/2022/2019/2015, and the Organizing Committee Vice Chair for the International Conference on Communications and Mobile Computing (CMC 2010). He acted as the Publicity Chair for several international conferences, such as the IEEE PIMRC 2012. He is the Principal Investigator for over 30 current or finished research projects, including the National Natural Science Foundation of China, the Science and Technology Program of Guangdong Province, and the Science and Technology Program of Shenzhen City. He is serving as an Associate Editor for IEEE TRANSACTIONS ON ANTENNAS AND PROPAGATION, IEEE TRANSACTIONS ON MOBILE COMPUTING, IEEE Antennas and Propagation Magazine, IEEE ANTENNAS AND WIRELESS PROPAGATION LETTERS, International Journal of Communication Systems China Communications, and Wireless Communications and Mobile Computing. He served as an Associate Editor for Security and Communication Networks journal and IEEE Network

George Goussetis (Senior Member, IEEE) received the Diploma degree in electrical and computer engineering from the National Technical University of Athens, Greece, in 1998, B.Sc. degree in physics (First Class) from University College London, U.K., in 2002, and the Ph.D. degree from the University of Westminster, London, U.K., in 2002.,In 1998, he joined the Space Engineering, Rome, Italy, as a RF Engineer and in 1999 the Wireless Communications Research Group, University of Westminster, U.K., as a Research Assistant. From 2002 to 2006, he was a Senior Research Fellow with Loughborough University, U.K. He was a Lecturer (Assistant Professor) with Heriot-Watt University, Edinburgh, U.K., from 2006 to 2009, and a Reader (Associate Professor) with Queen's University Belfast, U.K., from 2009 to 2013. In 2013, he joined Heriot-Watt as a Reader and was promoted to a Professor in 2014, where he currently directs the Institute of Sensors Signals and Systems. He has authored or coauthored over 500 peer-reviewed papers five book chapters one book and four patents. His research interests are in the area of microwave and antenna components and subsystems.,Dr. Goussetis has held a research fellowship from the Onassis foundation in 2001, a research fellowship from the U.K. Royal Academy of Engineering from 2006 to 2011 and European Marie-Curie experienced researcher fellowships in 2011 and 2012 and again in 2014 and 2017. He is the co-recipient of the 2011 European Space Agency Young Engineer of the Year Prize, the 2011 EuCAP Best Student Paper Prize, the 2012 EuCAP Best Antenna Theory Paper Prize, and the 2016 Bell Labs Prize. He has served as an Associate Editor for IEEE Antennas and Wireless Propagation Letters.

Guy A. E. Vandenbosch (Fellow, IEEE) received the M.S. and Ph.D. degrees in electrical engineering from Katholieke Universiteit Leuven, Leuven, Belgium, in 1985 and 1991, respectively.,From September to December 2014, he was a Visiting Professor with Tsinghua University, Beijing, China. Since 1993, he has been a Lecturer with Katholieke Universiteit Leuven, where he has been a Full Professor. His work has been published in ca. 400 articles in international journals and has led to ca. 425 papers at international conferences. His current research interests include in the area of electromagnetic (EM) theory, computational electromagnetics, planar antennas and circuits, nano-EMs, EM radiation, electromagnetic compatibility (EMC), and bio-EMs.,Dr. Vandenbosch has been a member of the "Management Committees" of the consecutive European COST actions on antennas since 1993. Within the ACE Network of Excellence of the EU from 2004 to 2007, he was a member of the Executive Board and coordinated the activity on the creation of a European antenna software platform. After ACE, from 2007 to 2018, he was the Chair of the EuRAAP Working Group on Software. He was a Vice-Chairman from 1999 to 2004, a Secretary from 2005 to 2009, and a Chairman from 2010 to 2017 of the IEEE Benelux Chapter on Antennas and Propagation. From 2002 to 2004, he was a Secretary of the IEEE Benelux Chapter on EMC. From 2012 to 2014, he was a Secretary of the Belgian National Committee for Radio-Electricity (URSI), where he is also an In-Charge of Commission. From 2017 to 2020, he was a member of the IEEE Electromagnetics Award Committee

Yi Huang (Fellow, IEEE) received the B.Sc. degree in physics from Wuhan University, Wuhan, China, in 1984, the M.Sc. (Eng.) degree in microwave engineering from the Nanjing Research Institute of Electronics Technology (NRIET), Nanjing, China, in 1987, and the D.Phil. degree in communications from the University of Oxford, Oxford, U.K., in 1994. His experience includes three years with NRIET, China, as a Radar Engineer; and various periods with the University of Birmingham, University of Oxford, and University of Essex, U.K., as a Research Staff Member. In 1994, he was a Research Fellow with the British Telecom Laboratories. In 1995, he joined as a Faculty Member with the Department of Electrical Engineering and Electronics, University of Liverpool, U.K., where he is currently a Full Professor of wireless engineering, the Head of the High Frequency Engineering Group, and the Deputy Head of the Department. He has authored or coauthored more than 400 refereed articles in leading international journals and conference proceedings and authored three books, including a bestseller Antennas: From Theory to Practice (John Wiley, 2008 and 2021). He has received many patents and research grants from research councils, government agencies, charities, the EU, and industry. His research interests include antennas, wireless communications, applied electromagnetics, radar, and EMC, with a current focus on mobile antennas, wireless energy harvesting, and power transfer. He was the U.K. and Ireland Representative of the European Association of Antenna and Propagation (EurAAP) (2016–2020) and a fellow of IET. He was a recipient of more than ten awards, such as the BAE Systems Chairman's Award 2017, the IET, and the best paper awards. He was on a number of national and international technical committees and has been an editor, an associate editor, or a guest editor of five international journals. He is the Editor-in-Chief of Wireless Engineering and Technology and an Associate Editor of IEEE TRANSACTIONS ON ANTENNAS AND PROPAGATION (2022 – now), and an Associate Editor of IEEE Antennas and Wireless Propagation Letters (2016 – 2022). In addition, he has been a Keynote/an Invited Speaker and an Organizer of many conferences and workshops, such as IEEE iWAT2010, LAPC2012, and EuCAP2018